A Family of Peroxo-titanate Materials Tailored for Optimal Strontium and Actinide Sorption

May Nyman*,† and David T. Hobbs*,‡

Sandia National Laboratories, P.O. Box 5800 MS 0754, Albuquerque, New Mexico 87185-0754, and Savannah River National Laboratory, Washington Savannah River Company, Aiken, South Carolina 29808

Received July 31, 2006. Revised Manuscript Received October 10, 2006

Achieving global optimization of inorganic sorbent efficacy, as well as tailoring sorbent specificity for target sorbates, would facilitate increased widespread use of these materials in applications such as producing potable water or nuclear waste treatment. Sodium titanates have long been known as sorbents for radionuclides, ^{90}Sr and transuranic elements in particular. We have developed a related class of materials, which we refer to as peroxo-titanates. These are sodium titanates or hydrous titanates synthesized in the presence of, or treated postsynthesis with, hydrogen peroxide. Peroxo-titanates show remarkable and universal improved sorption behavior with respect to separation of actinides and strontium from Savannah River Site (SRS) nuclear waste simulants. Enhancement in sorption kinetics can potentially result in as much as an order of magnitude increase in batch processing throughput. Peroxo-titanates have been produced by three different synthetic routes: postsynthesis peroxide treatment of a commercially produced monosodium titanate, an aqueous-peroxide synthetic route, and an isopropanol-peroxide synthetic route. The peroxo-titanate materials are characteristically yellow to orange, indicating the presence of protonated or hydrated Ti-peroxo species; the chemical formula can be generally written as $H_vNa_wTi_2O_5 \cdot (xH_2O)[yH_zO_2]$, where $(v + w) = 2$, $z = 0-2$, and total volatile species accounts for 25−50 wt % of the solid. Further enhancement of sorption performance is achieved by processing, storing, and utilizing the peroxo-titanate as an aqueous slurry rather than a dry powder and by postsynthesis acidification. All three synthesis modifications, addition of hydrogen peroxide, use of a slurry form, and acidification, can be applied more broadly to the optimization of other metal oxide sorbents and other ion separations processes.

Introduction

Inorganic sorbents for ion separations are applied in both industry and the public sector for sequestration of hazardous species, recovery of precious metals, and improvement of water quality and purity. Some specific applications include removal of radionuclides from nuclear wastes[1−5] and contaminated waste sites,[1,6] water softening,[7] arsenic removal from domestic water supplies,[8−11] treatment of industrial wastewater,[12,13] and scavenging trace metals from catalytic reaction products (i.e., pharmaceuticals).[14] Natural and synthetic clays,[15,16] zeolites[16,17] and other nanoporous frameworks,[18−20] micro-[21,22] and mesoporous[23] materials, and hydrous metal oxides[24,25] have all been shown to be effective in metal separation applications. Mechanisms of ion sorption can broadly be described as ion exchange on surfaces (especially with surface H^+) or in layers, channels, or pores; or as electrostatic binding of ions to oppositely charged

* Corresponding author. E-mail: mdnyman@sandia.gov (M.N.); david.hobbs@srnl.doe.gov (D.H.).
† Sandia National Laboratories.
‡ Savannah River National Laboratory.

(1) Sylvester, P.; Clearfield, A. *Solvent Extr. Ion Exch.* **1998**, *16*, 1527−1539.
(2) Sylvester, P.; Clearfield, A. *Sep. Sci. Technol.* **1999**, *34*, 2539−2551.
(3) Kumar, S. S.; Sivaiah, M. V.; Venkatesan, K. A.; Krishna, R. M.; Murthy, G. S.; Sasidhar, P. *J. Radioanal. Nucl. Chem.* **2003**, *258*, 321−327.
(4) Behrens, E. A.; Sylvester, P.; Clearfield, A. *Environ. Sci. Technol.* **1998**, *32*, 101−107.
(5) Song, Y. J.; Jiang, L. Q.; Zhao, A. M.; Jin, Q. X.; Song, D. K. *J. Radioanal. Nucl. Chem.* **1997**, *222*, 75−80.
(6) Marinin, D. V.; Brown, G. N. *Waste Manage.* **2000**, *20*, 545−553.
(7) Cinar, S.; Beler-Baykal, B. *Water Sci. Technol.* **2005**, *51*, 71−77.
(8) Dixit, S.; Hering, J. *Environ. Sci. Technol.* **2003**, *37*, 4182−4189.
(9) Manna, B.; Dasgupta, M.; Ghosh, U. C. *J. Water Supply: Res. Technol.−AQUA* **2004**, *53*, 483−495.
(10) Lenoble, W.; Laclautre, C.; Deluchat, W.; Serpaud, B.; Bollinger, J. C. *J. Hazard. Mater.* **2005**, *123*, 262−268.
(11) Lackovic, J. A.; Nikolaidis, N. P.; Dobbs, G. M. *Environ. Eng. Sci.* **2000**, *17*, 29−39.
(12) El-Kamash, A. M.; Zaki, A. A.; Geleel, M. A. E. *J. Hazard. Mater.* **2005**, *127*, 211−220.
(13) Hui, K. S.; Chao, C. Y. H.; Kot, S. C. *J. Hazard. Mater.* **2005**, *1−3*, 89−101.
(14) Garrett, C. E.; Prasad, K. *Adv. Synth. Catal.* **2004**, *346*, 889−900.
(15) Scheidegger, A. M.; Strawn, D. G.; Lamble, G. M.; Sparks, D. L. *Geochim. Cosmochim. Acta* **1998**, *62*, 2233−2245.
(16) Bailey, S. E.; Olin, T. J.; Bricka, R. M.; Adrian, D. D. *Water Res.* **1999**, *33*, 2469−2479.
(17) Kesraouiouki, S.; Cheeseman, C. R.; Perry, R. *J. Chem. Technol. Biotechnol.* **1994**, *59*, 121−126.
(18) Walcarius, A.; Ganesant, V. *Langmuir* **2006**, *22*, 469−477.
(19) Wang, X. L.; Gao, Q. M.; Wu, C. D.; Hu, J.; Ruan, M. L. *Microporous Mesoporous Mater.* **2005**, *85*, 355−364.
(20) Pinnavaia, T. J. *Mater. Chem.* **1995**, *245*, 283−300.
(21) Clearfield, A.; Wang, Z. K. *J. Chem. Soc., Dalton. Trans.* **2002**, 2937−2947.
(22) Rocha, J.; Lin, Z. *Micro- Mesopor. Miner. Phases* **2005**, *57*, 173−201.
(23) Moller, K.; Bein, T. *Chem. Mater.* **1998**, *10*, 2950−2963.
(24) Moller, T.; Clearfield, A.; Harjula, R. *Microporous Mesoporous Mater.* **2002**, *54*, 187−199.
(25) Moller, T.; Harjula, R.; Kelokaski, P.; Vaaramaa, K.; Karhu, P.; Lehto, J. *J. Mater. Chem.* **2003**, *13*, 535−541.

10.1021/cm061797h CCC: $33.50
Published on Web 11/18/2006

surface sites. Understanding and optimizing selectivity, kinetics, and capacity of sorbent materials for specific ions under varying chemical environments is the ultimate challenge for researchers who seek improved performance of ion-exchange materials.

Whereas the counterpart organic phases for ion sequestration such as calixarenes enjoy the advantage of precise atomic control over size and functional groups that define the ion sequestering cavity, they suffer from lack of stability in harsh chemical or radiological environments, such as those found in nuclear wastes. Contrarily, precise design of inorganic sorbents is somewhat hampered by thermodynamic or kinetic limitations of metal oxide systems; but inorganic sorbents are superior in their ability to withstand harsh chemical environments. Organic sequestering reagents are generally difficult to synthesize with multiple-step and low-yield processes, whereas inorganic sorbents such as metal oxides are produced in high yields by simple reactions, and they occur naturally (zeolites, clays). Liu et al.[26,27] introduced a class of sorbents that features metal oxide scaffolds functionalized with self-assembled monolayers of sorbate-specific ligands. Although this elegant approach provides the rugged substrate of inorganic materials with the selectivity or specificity of organic functional groups, it still lacks the simplicity and stability that is preferred for some applications such as water treatment or nuclear waste processing.

Control over specificity or selectivity of inorganic sorbent materials is in fact a challenge that has infrequently been demonstrated. Size matching the targeted sorbate to the sorption site in a porous phase is one approach to tailoring ion selectivity, exemplified by crystalline silicotitanate (CST, $Na_2Ti_2SiO_7 \cdot 2H_2O$). CST is a zeotype phase with high selectivity for Cs^+ (for sequestration of radioactive ^{137}Cs) because of the ideal size-matching of the exchange sites in the pores.[28,29] Furthermore, the selectivity of CST for Cs^+ is improved by substituting Nb^{5+} into 25% of the framework Ti^{4+}.[28] The improved selectivity is rationalized by the charge-compensating replacement of 25% of the channel Na^+ with water, which both provides additional coordination and thus stabilization of Cs^+ and results in less repulsion between neighboring cations in the channel.[30,31] Furthermore, the replacement of Ti with Nb slightly increases the unit cell size, and the larger tunnel more readily accommodates transport of cesium to binding sites.[31] However, the drawback of a size-exclusion approach such as that present in the one-dimensional tunnels of CST is slow sorption kinetics and relatively low ion exchange capacity.

We are interested in developing optimized, titanate-based inorganic sorbents without necessarily adding great expense or difficulty to production. Although we anticipate more widespread applicability of our optimized sorbents, we specifically target removal of ^{90}Sr and alpha-emitting radionuclides, principally $^{238,239,240}Pu$ and ^{237}Np, from the highly alkaline wastes that derive from reprocessing of irradiated fuel and target materials at the Savannah River Site (SRS).

Presently, the SRS has identified monosodium titanate (MST) for Sr and actinide separations in the Actinide Removal Process (ARP) facility and the Salt Waste Processing Facility (SWPF) via a batch contact method.[32] Monosodium titanate, which was first developed by Dosch[33] at Sandia National Laboratories as a radionuclide sorbent, is a poorly crystalline, layered sodium titanate with an approximate chemical formula of $HNaTi_2O_5 \cdot xH_2O$. SRNL researchers modified the synthesis of the MST to produce a spherical morphology with $\sim 0.5-2\ \mu$m diameter tailored for use at the SRS.[32] A more crystalline version of sodium titanate known as sodium nonatitanate ($Na_4Ti_9O_{20} \cdot xH_2O$) has also been assessed to have suitable sorption capabilities for nuclear waste treatment applications.[1,2,34] SrTreat is a commercially available titanate-based ion exchanger that has noteworthy selectivity for strontium in nuclear waste media.[35]

Titanate-based materials offer the advantages of robustness in harsh chemical and radioactive environments, ease of synthesis, and effective sorption capabilities in a variety of media, including acidic, basic, and neutral and high or low ionic strength. Whereas all variations of these titanate sorbents have been shown to have sufficient strontium-removal capabilities, they lack suitable kinetics and selectivity for actinide separations (Pu in particular).

We report here a general synthetic strategy for any titanate-based sorbent (including mixed metal titanates such as silicotitanates) that results in significantly improved sorption characteristics. The addition of hydrogen peroxide, either during formation of the titanate material or as a posttreatment step, results in formation of a peroxo-titanate,[36] which is identified by its characteristic yellow color, indicative of hydrated or protonated Ti-peroxo bonds.[37,38] Further improvements in sorption capabilities are imparted by (1) postsynthesis acidification of the peroxo-titanate materials and (2) utilizing the sorbents as slurries rather than as dry powders.

Three synthetic routes for peroxo-titanate materials are reported in this paper, all of which show significantly

(26) Fryxell, G. E.; Lin, Y.; Fiskum, S.; Birnbaum, J. C.; Wu, H. *Environ. Sci. Technol.* **2005**, *39*, 1324−1331.
(27) Fryxell, G. E.; Liu, J.; Mattigod, S. *Mater. Technol.* **1999**, *14*, 188−191.
(28) Anthony, R. G.; Dosch, R. G.; Philip, C. V. Method of Using Novel Silico-titanates. U.S. Patent 6 110 378, Sandia National Laboratories, 2000.
(29) Anthony, R. G.; Philip, C. V.; Dosch, R. G. *Waste Manage.* **1993**, *13*, 503.
(30) Cherry, B. R.; Nyman, M.; Alam, T. M. *J. Solid State Chem.* **2004**, *177*, 2079−2093.
(31) Tripathi, A.; Medvedev, D. G.; Nyman, M.; Clearfield, A. *J. Solid State Chem.* **2003**, *175*, 72−83.
(32) Hobbs, D. T.; Barnes, M. J.; Pulmano, R. L.; Marshall, K. M.; Edwards, T. B.; Bronikowski, M. G.; Fink, S. D. *Sep. Sci. Technol.* **2005**, *40*, 3093−3111.
(33) Dosch, R. G. *Use of Titanates in Decontamination of Defense Waste*; Report RS-8232−2./50318; Sandia National Laboratories: Albuquerque, NM, 1978.
(34) Behrens, E. A.; Sylvester, P.; Clearfield, A. *Environ. Sci. Technol.* **1998**, *32*, 101−107.
(35) Lehto, J.; Brodkin, L.; Harjula, R.; Tusa, E. *Nucl. Technol.* **1999**, *127*, 81−87.
(36) Nyman, M. D.; Hobbs, D. T. Hydrogen Peroxide Modified Sodium Titanates with Improved Sorption Capabilities. U.S. patent application #SD-7976; Sandia National Laboratories, submitted May 2005.
(37) Bonino, R.; Damin, A.; Ricchiardi, G.; Ricci, M.; Spano, G.; D'Aloisio, R.; Zecchina, A.; Lamberti, C.; Prestipino, C.; Bordiga, S. *J. Phys. Chem. B* **2004**, *108*, 3573−3583.
(38) Bordiga, S.; Damin, A.; Bonino, F.; Ricchiardi, G.; Zecchina, A.; Tagliapietra, R.; Lanberti, C. *Phys. Chem. Chem. Phys.* **2003**, *5*, 4390−4393.

improved sorption performance over their related titanate materials. The three synthetic routes explored in this study include (1) postsynthesis peroxide treatment of MST, (2) isopropanol-peroxide synthesis, and (3) aqueous-peroxide synthesis. Synthesis, characterization, and radionuclide separation studies for the peroxo-titanate materials are described in this report. Preliminary evaluation of the peroxide-modified MST materials for treatment of SRS high-level waste demonstrates remarkable improvement in processing efficiency. The increased capacity and kinetics exhibited by the peroxo-titanates suggest that the use of these materials should increase the throughput of the processing facilities resulting in significant operating and life-cycle cost savings.

Experimental Section

Synthesis of Peroxo-titanates. *Postsynthesis Peroxide Treatment of MST Slurry.* MST slurry (Optima Chemical Group Ltd, Lot 00-QAB-417) containing 14.8 wt % MST solids, pH ~10.8) slurry was used for all posttreatment preparations. Table 1 provides a summary of the peroxide treatment conditions. Variations in treatment conditions included H_2O_2:Ti ratio, pH of the MST slurry, contact time of the slurry with the peroxide solution, and post-peroxide treatment pH adjustment. Generally, 10 g of MST slurry was stirred in a small glass beaker and the pH of the MST slurry was decreased using 0.1−2 M nitric acid solutions. Hydrogen peroxide solution (30 wt %) was added dropwise to the MST slurry to obtain the desired H_2O_2:Ti ratio. Upon addition of the hydrogen peroxide, the white MST immediately changes to a bright yellow color and is accompanied by the evolution of oxygen gas bubbles. Some dissolution of the MST occurred during this process, as indicated by the yellow color of the aqueous portion of the slurry. After the appropriate contact time, the peroxide remaining in solution was removed by subsequent filtering and washing of the solids with fresh deionized, distilled water, without complete drying of the sample. For experiments 13P and 14P, a final pH adjustment was made by adding 0.1 M nitric acid solution until the desired pH was reached.

Isopropanol-peroxide Route. These syntheses were derived from the MST synthesis developed by Hobbs et al.[32] Synthesis parameters varied for these experiments included H_2O_2:Ti ratio, mixing time, acidic or neutral H_2O for hydrolysis and condensation of alkoxides, and postsynthesis pH adjustments. Synthesis parameters are summarized in **Table 1**. The peroxo-titanate phases from these syntheses were either filtered and air-dried to obtain a dry powder or converted to an aqueous slurry and, if appropriate, pH-adjusted as described above. A typical preparation is described in detail as follows. Titanium isopropoxide (TIPT, $Ti(OC_3H_7)_4$, 1 g, 3.5 mmol) and sodium methoxide ($NaOCH_3$, 0.095 g, 1.75 mmol) are placed in a 20 mL glass vial containing a stirbar in an inert atmosphere box to give a 1:2 Na:Ti ratio. The vial is capped and transferred outside the glovebox, where 9 mL of isopropanol is pipetted into the vial. The mixture is stirred until a clear, pale yellow solution is obtained. In a separate vial, 30 wt % H_2O_2 solution (i.e., 1.2 g, 10.5 mmol H_2O_2 for 3:1 H_2O_2:Ti ratio) is combined with 1 g of water or 1 g of 0.1 M nitric acid solution (referred to as neutral or acidic, respectively, in Table 1). This aqueous solution is then added to the isopropanol solution and a yellow precipitate forms instantaneously; stirring is continued for the predetermined time. Typical yield is 0.35−0.40 g of dry yellow powder. ***Cautionary note****: this reaction evolves gas from decomposition of the H_2O_2. Do not tightly cap vials during the reaction; pressure build-up will break the vials!*

Aqueous-peroxide Route, Basic (Experiments 1A−14A). This synthetic procedure can generally be described as dissolution of titanium alkoxide in a hot, strongly alkaline H_2O_2 solution followed by precipitation of the titanate material. Variables in these syntheses included molar concentration of sodium hydroxide, ratio of H_2O_2:Ti, and postacidification of the product. Other experimental parameters investigated included utilizing the final sorbent product as a powder vs a slurry, a secondary posttreatment with H_2O_2, use of $TiCl_4$ instead of titanium ispopropoxide as a Ti precursor, and reverse order of Ti and H_2O_2 addition. A typical synthesis is described as follows (experiment 1A). Sodium hydroxide solution (3 M, 75 mL) is heated and stirred in a 125 mL Erlenmeyer flask. When the solution reaches around 60 °C, 6 g (21 mmol) of TIPT is added from a pipet to the hot solution, whereupon a white precipitate immediately forms. Approximately 40 g of 30 wt % H_2O_2 solution is added slowly, around 10 g at a time. The addition of the H_2O_2 results in dissolution of the white precipitate to obtain a bubbly, clear, bright yellow solution. Continued stirring and heating of the solution (approximately 10−60 min) results in precipitation of a yellow solid. Either a dry powder is obtained by vacuum filtration and rinsing with DI water, or a slurry is obtained by multiple cycles of decanting the reaction solution and replacing it with fresh DI water. ***Cautionary note****: In strongly basic solutions, H_2O_2 decomposes rapidly and exothermically with gas evolution. Be alert for solution boil-over.*

Synthesis from $TiCl_4$ (Experiment 8A). Sodium hydroxide solution (25 mL, 16 M NaOH) is placed in a 100 mL flask. While stirring the solution at room temperature, we add 45 mL of 0.09 molar $TiCl_4$, 20% HCl aqueous solution (Aldrich) via syringe. A grayish precipitate is observed. Twenty grams of 30 wt % H_2O_2 solution is slowly added. Over the course of peroxide addition, the solution becomes clear yellow and then precipitates a greenish-yellow solid, which is collected by vacuum filtration. Yield = 0.49 g. ***Cautionary note****: this reaction is very exothermic; it should be carried out in a fumehood and executed with caution.*

Synthesis from $TiCl_4$ with Reverse Addition of Reagents (Experiment 7A). Twenty grams of 30 wt % H_2O_2 solution is placed in a 100 mL Erlenmeyer flask. Seventeen milliliters of a 0.09 M $TiCl_4$, 20% HCl aqueous solution is added via syringe, resulting in a bright orange solution. While the solution is stirred, 3 M NaOH solution is added dropwise. After about 10 mL is added, a yellow precipitate was formed and no more NaOH was added. Yield: 0.17 g.

Second Postsynthesis Peroxide Treatment (Experiments 12A & 13A). After a yellow precipitate is formed from the TIPT/NaOH/H_2O/H_2O_2 mixture (basic aqueous peroxide route), the precipitate is left to settle. The liquid is decanted, more DI water is added, the mixture is stirred, and this process is continued until the decanted liquid no longer appears yellow. More DI water is added to bring the total volume to around 200 mL. Ten grams of 30 wt % H_2O_2 solution is added, and the slurry is stirred for about 20 min (note: prolonged stirring results in complete dissolution of the precipitate). The decantation process is repeated as described above. Centrifugation of the slurry prior to decanting was utilized in this case because the solids settle more slowly after the second peroxide treatment.

Aqueous-peroxide Route, Acidic (Experiments 14A−17A): Experiments 14A and 15A. Six milliliters of 15.8 M nitric acid solution was added to 94 mL of DI water to obtain 100 mL of ~1 M nitric acid solution. For 15A, 0.6 g (7.0 mmol) of sodium nitrate was dissolved in the nitric acid solution. While the solution was heated and stirred, 2 g of TIPT (7.0 mmol) was added dropwise to form a deep red, clear solution. Each solution was boiled down to ~20 mL. Sodium hydroxide solution (2 molar) was added gradually; the red color faded and a yellow solid precipitated. The final pH for experiment 14A was 8.8 and the final pH for experiment 15A was 11.7.

Table 1. Summary of Synthesis Parameters for Peroxo-titanate Materials

Postsynthesis Peroxide Treatment of Optima MST Slurry

experiment no.	H_2O_2:Ti ratio	pH of H_2O_2 treatment	contact time (h)	final pH adjustment	product composition[e] (Ti:Na molar ratio)
1P	3.0	2	24	no	17.3
2P	3.0	3	24	no	9.43
3P	3.0	4	24	no	5.63
4P	3.0	5	24	no	4.19
5P	3.0	6	24	no	3.38
6P	3.0	7	24	no	3.34
7P	3.0	8	24	no	2.87
8P	0.3	4	24	no	5.93
9P	1.0	4	24	no	5.82
10P	6.0	4	24	no	5.83
11P	3.0	4	4	no	6.08
12P	3.0	4	96	no	4.97
13P	3.0	7	24	yes (pH 2)	3.45
14P	3.0	7	24	yes (pH 4)	3.39
15P	6.0[a]	4	24	no	6.06

Isopropanol-Peroxide Route

						product composition[e]	
experiment no.	H_2O_2:Ti ratio	neutral/acidic[b]	contact time (h)	final pH adjustment	powder or slurry	wt % volatile[d]	Ti:Na molar ratio
1I	3.0	neutral	24	no	powder	30	2.12
2I	3.0	neutral	96	no	powder	28	2.13
3I	0.3	neutral	24	no	powder	48	1.96
4I	1.0	neutral	24	no	powder	35	1.64
5I	6.0	neutral	24	no	powder	30	2.05
6I	3.0	acidic	24	no	powder	29	2.07
7I	3.0	acidic	4	no	powder	32	1.60
8I	3.0	neutral	24	yes (pH 2)	powder	32	40.8
9I	3.0	neutral	24	yes (pH 4)	powder	32	23.1
10I	3.0	neutral	24	no	slurry	32	2.17
11I	3.0	acidic	24	no	slurry	36	1.94
12I	3.0	neutral	24	yes (pH 4)	slurry	30	22.4
13I	3.0	acidic	24	yes (pH 4)	slurry	35	36.5

Aqueous-Peroxide Route

					product composition[e]	
experiment no.	aqueous solution for synthesis	powder or slurry	final pH adjustment	other conditions	wt % volatile[d]	Ti:Na molar ratio
1A	3 M NaOH	powder	no		23	1.67
2A	2 M NaOH	powder	no		24	1.75
3A	1 M NaOH	powder	no		26	1.55
4A	3 M NaOH	powder	yes (pH 2)		43	27.1
5A	3 M NaOH	powder	yes (pH 4)		48	7.37
6A	3 M NaOH	powder	no	1/2 concentration of Ti in base	28	1.93
7A	3 M NaOH	powder	no	$TiCl_4$ in place of TIPT, inverse addition of reagents[c]	33	1.55
8A	3 M NaOH	powder	no	$TiCl_4$ in place of TIPT, normal addition of reagents[c]	36	1.58
9A	3 M NaOH	powder	no	1/10 concentration of Ti in base	53	1.83
10A	3 M NaOH	slurry	no		25	2.07
11A	3 M NaOH	slurry	yes (pH 4)		25	6.68
12A	3 M NaOH	slurry	no	second postsynthesis peroxide treatment (see text)	24	2.04
13A	3 M NaOH	slurry	yes (pH 4)	second postsynthesis peroxide treatment (see text)		5.79
14A	1 M HNO_3	slurry	no	2 M NaOH added to precipitate titanate product (see text)		23.2
15A	1 M HNO_3 & $NaNO_3$	slurry	no			3.16
16A	1 M HNO_3	slurry	yes (pH 4)			46.5
17A	1 M HNO_3 & $NaNO_3$	slurry	yes (pH 4)			5.51

[a] This preparation employed 2 sequential 24 h contacts of MST with hydrogen peroxide at a 3:1 mole ratio. [b] We added 2.2 g of water/H_2O_2 alcohol solution for hydrolysis and condensation of Na and Ti alkoxides. Acidic refers to 0.1 M nitric acid solution (see text). [c] Normal addition: Ti added to base, followed by the addition of peroxide. Inverse addition: Ti added to peroxide, followed by the addition of base. [d] The weight percent volatile was determined by the TGA weight loss of volatile species of dry powder (OH^-, H_2O, H_2O_2, H_3O^+, H_2O_2, HOO^-, O_2^{2-}, etc.). [e] The composition for dry powder, in the case of a slurry product.

Table 2. Composition of Simulated Waste Solution

component	target concentration	measured concentration[a]
$NaNO_3$	2.60 M	2.44 (0.24) M
NaOH	1.33 M	1.36 (0.14) M
Na_2SO_4	0.521 M	0.551 (0.055) M
$NaAl(OH)_4$	0.429 M	0.503 (0.050) M
$NaNO_2$	0.134 M	0.116 (0.012) M
Na_2CO_3	0.0260 M	0.016 (0.010) M
total Na	5.6 M	5.2 (0.52) M
total Sr	0.6 mg L^{-1}	0.484 (0.032) mg L^{-1}
^{85}Sr	>1000 dpm mL^{-1}	1.65 × 105 (3.22 × 103) dpm mL^{-1} [b]
total Pu	0.2 mg L^{-1}	0.218 (0.013) mg L^{-1}
^{237}Np	0.5 mg L^{-1}	0.461 (0.090) mg L^{-1}
total U	10 mg L^{-1}	9.55 (0.33) mg L^{-1}

[a] Numbers in parenthesis are the analytical uncertainty of reported value. [b] Value at the time solution was first prepared. ^{85}Sr has a 64.8 day half-life and, therefore, the ^{85}Sr activity in the solution is continuously decreasing.

Acidification of Peroxo-titanates. Powder: Approximately 0.2 g of peroxo-titanate powder is placed in 150 mL of water and stirred. Nitric acid solution (0.1 M) is slowly added dropwise until the desired pH is reached (generally 2, 4, or 5). The powder is collected by vacuum filtration. Slurry: The as-prepared slurry is stirred while 0.1 M nitric acid solution is added dropwise until the desired pH is obtained. The pH-adjusted slurry requires no further modification.

Characterization of Peroxo-titanates. *Instrumentation.* The peroxo-titanates were characterized by a number of techniques, including powder X-ray diffraction (XRD), scanning electron microscopy (SEM), thermogravimetric analysis−differential thermal analysis (TGA−DTA), infrared spectroscopy (IR), compositional analysis (Na and Ti), high-resolution transmission electron microscopy (HR-TEM), and surface area analysis. X-ray diffraction was performed with a Bruker D8 Advance Diffractometer in Bragg−Brentano geometry with Ni-filtered Cu−Kα radiation. Samples were examined with a JEOL JSM-6300V scanning electron microscope (SEM) equipped with a Link GEM Oxford detector and IRIDIUM IXRF Systems software for EDAX analysis. Transmission electron microscopy (TEM) was done with a Philips CM 30 TEM operating at 300 kV accelerating voltage, and powder samples were salted onto a carbon-coated copper TEM grid.

Thermal analysis was performed with a TA Instruments SDT 2960 simultaneous TGA−DTA under a nitrogen flow with a heating rate of 5 °C/min. Infrared spectra (400−4000 cm^{-1}) were recorded on a Perkin-Elmer Spectrum GX FTIR using the KBr pellet method. Surface area measurements were obtained by BET analysis of adsorption isotherms on a Quantachrome Autosorb-1 or Micromeritics ASA2010 Porosimeter Analyzer. Nitrogen was used as the adsorbate, and samples were outgassed under a vacuum at room temperature overnight prior to analysis. Micropore surface areas were determined by T-plot analysis; average pore diameter and pore volume were obtained via BJH analysis of desorption isotherms.

Compositional Analysis. The sodium and titanium contents for each sample were determined by inductively coupled plasma atomic emission spectroscopy using a Perkin-Elmer Optima 3000 instrument. Samples were first dissolved in 3 M sulfuric acid solution and diluted 20:1 in 2% nitric acid solution.

Performance Testing with Simulated Waste Solution. Testing of combined strontium and actinide removal performance was carried out at the Savannah River National Laboratory (SRNL) using the simulated waste solution composition as shown in Table 2, including plutonium, uranium, and neptunium in addition to ^{85}Sr. Strontium and actinide removal testing occurred at 25 ± 3 °C at an equivalent MST solids concentration of 0.4 g/L. Standard sampling of the test bottles occurred at 4, 24, and 168 h of contact. Additional interim samplings between 4 and 24 h were taken for select tests to provide additional data on adsorption kinetics. Samples were filtered through 0.45 μm syringe filters (nylon membrane) to remove MST solids. Gamma spectroscopy measured the ^{85}Sr and neptunium content. ^{85}Sr activities were decay corrected to the time of sampling. We measured the ^{238}Pu and $^{239,240}Pu$ content by radiochemical separation of the plutonium from uranium and neptunium followed by alpha counting of the extracted plutonium. Sorption tests using the baseline MST sample (Optima batch 00-QAB-417) and blank tests were run in parallel for comparison to the peroxo-titanate sorption tests and to confirm that loss of strontium and actinides did not occur by sorption onto container walls or filter surfaces.

Results and Discussion

Synthesis and Characterization of Peroxo-titanates. All peroxo-titanates synthesized in this study have the characteristic yellow color indicative of a titanium-peroxo species that is protonated or associated with water protons.[37,38] Generally, deeper yellow-orange hues were observed for acidified peroxo-titanate powders and slurries, and peroxo-titanate materials precipitated under alkaline conditions are pale yellow. For the isopropanol-peroxide syntheses, earlier studies indicated that base catalysis for hydrolysis and condensation of the alkoxide (as apposed to neutral or acidic, experiments 1I−13I) produced a less effective sorbent, so this route was not pursued further.

We generally obtained ∼80% yield or greater for the isopropanol-peroxide synthetic routes. Lower yields were obtained by the basic aqueous-peroxide routes because of partial dissolution of the product. We observed decreasing yields in the aqueous-peroxide route with increasing hydroxide concentration. Postsynthesis acidification and second peroxide treatments also decreased the product yields, again because of partial dissolution of the sorbent in these conditions. Although we observe dissolution of the peroxo-titanate materials in these harsh synthetic or postsynthetic treatment media, they do not exhibit significant solubility in the highly basic, high-ionic-strength simulant solutions. This suggests that excess hydrogen peroxide in the synthesis mixture is largely responsible for dissolution of the titanate powders.

Structure and Morphology of Peroxo-titanates. Generally, all the peroxo-titanate materials reported here appear amorphous by powder X-ray diffraction. Scanning Electron Micrographs (SEM) of the three types of peroxo-titanate materials are shown in Figure 1. The peroxide-treated MST materials appear identical to the original MST materials; spherically shaped (0.5−2 μm diameter) with a layered morphology on the particle surfaces. The peroxo-titanates synthesized in isopropanol media are largely featureless at the resolution of the SEM. The peroxo-titanates synthesized in aqueous NaOH consist entirely of entangled nanofibers. The acidic-aqueous route produced smooth, uniform spherical particles with a diameter similar to that of MST.

Transmission electron microscopy (TEM) was necessary to obtain more detailed morphological and possibly structural information from all three types of peroxo-titanates, given the poor long-range atomic ordering and the small scale of the observed morphological features. TEM images of cross-sectioned (via microtoming) MST spherical particles were

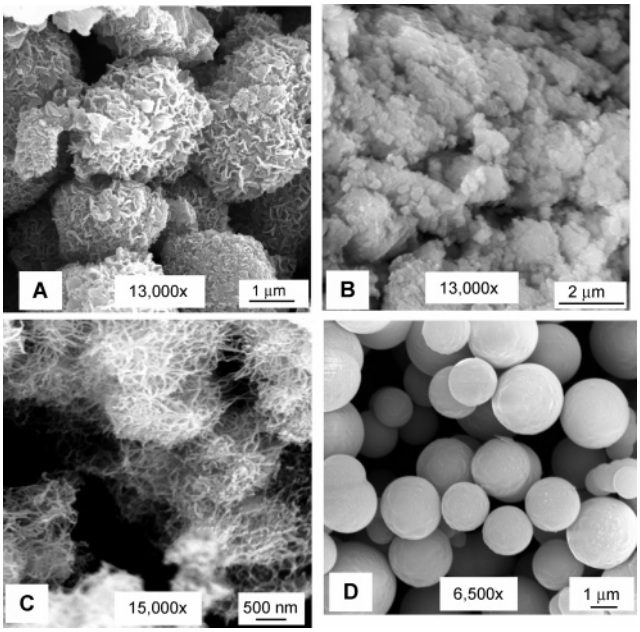

Figure 1. Scanning electron micrographs of (A) peroxide-treated MST, (B) peroxo-titanate from the isopropanol-peroxide synthesis, (C) peroxo-titanate from basic aqueous-peroxide synthesis, and (D) peroxo-titanate from acidic aqueous-peroxide synthesis.

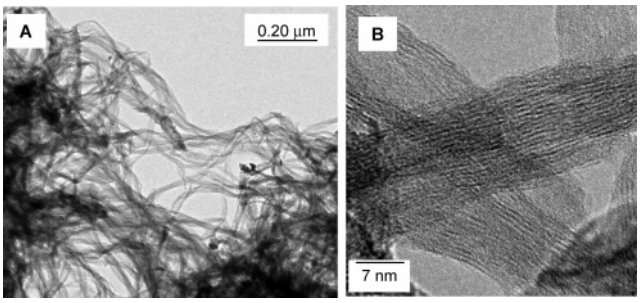

Figure 2. (A) Transmission electron micrograph. (B) High-resolution transmission electron micrograph of peroxo-titanate sorbent from the basic aqueous-peroxide synthesis, showing the fibrous morphology and the ~7−8 Å layers.

reported by Duff et al.[39] The TEM images revealed a fibrous and layered material with a layer-spacing around 6.3 Å.[39] However, this morphology resided only on the outer portion of the particles. The interior of the MST had no visible features.

The TEM and high resolution (HR) TEM images of peroxo-titanates produced by the basic aqueous syntheses reveal a layered structure within the fibers with a layer spacing of around 7−8 Å (Figure 2). The fibers are actually better described as ribbons and are generally less than 10 nanometers thick and 40 nanometers wide. The layer spacing observed in both the rims of the MST particles and in the fibrous peroxo-titanate materials formed via the aqueous-peroxide synthesis is similar to that observed in the more crystalline sodium nonatitanate.[40] This suggests that these aqueous peroxo-titanate materials (as well as the outer portion of MST) are similar in structure to that of sodium nonatitanate, but with much less long-range order or smaller particle size.

(39) Duff, M. C.; Hunter, D. B.; Hobbs, D. T.; Fink, S. D.; Dai, Z.; Bradley, J. P. *Environ. Sci. Technol.* **2004**, *38*, 5201−5207.
(40) Clearfield, A.; Lehto, J. *J. Solid State Chem.* **1988**, *73*, 98−106.

Sodium nonatitanates, which are processed hydrothermally at >100 °C for several days,[40] usually have sufficient long-range order to observe the layer spacing by X-ray powder diffraction. The MST and peroxo-titanates from the aqueous-peroxide route, both processed around 80 °C for 1−2 h, are amorphous by X-ray powder diffraction, but basal lattice planes can be easily observed and measured by HR-TEM. The peroxo-titanates from the isopropanol-peroxide route are processed at room temperature, and no crystalline features are observable by TEM.

Composition of Peroxo-titanates. The sodium:titanium ratios and wt % volatile species for the peroxo-titanate powders are compiled in Table 1. Generally, more weight loss due to volatile species is observed in post-acid-treated samples. This is a result of replacement of sodium with hydrated protons (H_3O^+, $H_5O_2^+$, etc.). The replacement of sodium with protons is also reflected in the compositions, with Ti:Na ratios ranging from 3 to 40, compared to values closer to 2 for the parent material. Peroxide treatment of MST (1P-15P) in acidic media also reduced the amount of sodium in the sorbent. Generally, a postsynthesis acidification or peroxide treatment at pH ~2−4 resulted in a material with Ti:Na > 20.

Because these peroxo-titanate materials are amorphous and, therefore, poorly defined, we can describe their chemical formulas only generally as $H_vNa_wTi_2O_5{\cdot}(xH_2O)[yH_zO_2]$ where $(v + w) = 2$. For peroxo-titanates synthesized under neutral or basic conditions, $v \approx w \approx 1$. For acid-treated peroxo-titanates, $v > w$. The species in square brackets is peroxide, which is most likely coordinated to the titanium and may be present as O_2^{2-}, HO_2^-, or H_2O_2 ($z = 0-2$).

The number of protons associated with the peroxide increases with increased acidification of the sample, as indicated by the deepening of the yellow hue. Representative TGA−DTA (thermogravimetry−differential thermal analysis) plots are shown in Figure 3. Generally, total weight loss varied from 25 to 50%. Figure 3a compares MST to peroxide-modified MST. The TGA−DTA plots showed a distinct weight loss event around 600 °C (~2−3 wt %) that is observed in virtually all of the peroxo-titanate materials that have not been acidified postsynthesis (see also panels b and c of Figure 3). This event is not observed with the MST sample. We attribute this event to the loss of the deprotonated peroxide groups.

Loss of protonated peroxide groups in the acidified peroxo-titanates appears to take place at a lower temperature, because for these acidified samples, there is more extensive weight loss below 300 °C and the weight-loss event at 600 °C is not apparent. The weight-loss event at 600 °C is accompanied by an exothermic phase change, as indicated by the DTA spectra (most apparent in panels a and c of Figure 4), and the baseline MST also has this exothermic event at 600 °C. In the acidified peroxo-titanate samples, the exothermic event occurs at 400 °C (panels b and c of Figure 5). This phase change is most likely crystallization of TiO_2 (anatase), which is observed in powder X-ray diffraction spectra of the sample, post-TGA−DTA analysis.

Peroxo-titanate Performance for Sr, Np, and Pu Sorption. The first set of results discussed is presented as

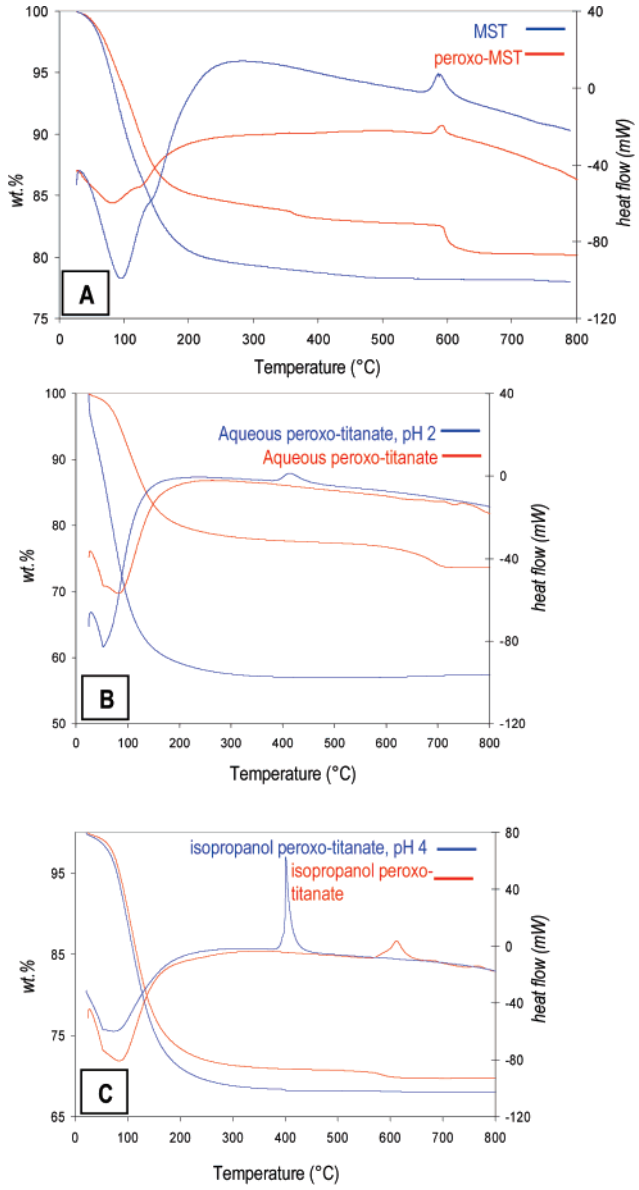

Figure 3. Thermogravimetric-differential thermal analysis (TGA-DTA) of (A) MST and peroxide-treated MST; (B) peroxo-titanate from basic aqueous-peroxide synthesis, and peroxo-titanate from basic aqueous-peroxide synthesis with postsynthesis acidification.; (C) peroxo-titanate from isopropanol-peroxide synthesis, and peroxo-titanate from isopropanol-peroxide synthesis with postsynthesis acidification.

normalized decontamination factors (DF). A decontamination factor is a unitless value defined as the ratio of the original sorbate concentration in solution (before treatment) to the concentration after contact with the sorbent. Normalization is achieved by dividing the decontamination factor of the peroxo-titanate by the decontamination factor for the baseline MST. Therefore, if the sorbent has a normalized DF >1, it is more effective than the baseline MST. Average Sr, Pu, and Np DF values measured with the simulated waste solution (Table 2) contacted with MST for 4 h are 64, 4.8, and 1.3, respectively.

The bar graphs in Figure 4 summarize the normalized Sr, Np, and Pu DF values for the peroxide-modified MST samples (yellow), the peroxo-titanates from the isopropanol-synthesis (green), and the peroxo-titanates from the aqueous synthesis (blue), each with a 4 h contact time with the simulated waste solution. The red line across each graph represents the baseline MST performance, which by definition is unity. In general, every peroxo-titanate sorbent outperformed or matched the performance of MST for Sr, Pu, and Np removal. The peroxide-treated MST showed more consistent performance for the different sorbent preparations than those synthesized from the aqueous-peroxide or isopropanol-peroxide routes. This is predominantly due to the wider range of synthesis parameters explored for the aqueous-peroxide and isopropanol-peroxide synthetic routes, especially preparation of dry powders in addition to slurries.

Sorption was generally better for the slurries (10I−13I and 10A−17A) than for the analogous powder samples (1I−9I and 1A−9A). However, this trend was more evident for Pu and Sr than for Np (discussed below). Acidification of the peroxo-titanate as a postsynthesis step usually resulted in enhanced performance (especially for Sr and Pu); for instance, see 6P vs 13P, 10I vs 12I, and 12A vs 13A. However, the drawbacks of acidification include an additional processing step and loss of sorbent due to partial dissolution.

Figure 5 provides a summary of the top two performing sorbents of each of the three peroxo-titanate preparation types and the three radionuclides. Again, the data are based on 4 h DF values, normalized to MST. The most marked improvements over MST sorption capabilities are for Pu sorption, followed by Sr sorption, and comparably moderate improvements were observed for Np sorption.

Peroxo-titanates prepared by the aqueous route were the top two performers for each radionuclide. More specifically, each of the six aqueous-route peroxo-titanate sorbents highlighted in this graph is a slurry, with the exception of sample 7A, for Np sorption. Sample 13A was the best sorbent for Sr and Np, and the second best for Pu. This preparation method, however, involves three steps: initial precipitation of the peroxo-titanate, second postsynthesis peroxide treatment, and final acidification. Therefore, use on an industrial scale would require optimization of the synthesis process to minimize material loss by dissolution at each step.

Use of titanium chloride instead of the titanium alkoxide, inverse order of reagent addition, and reduction of Ti concentration (experiments 6A−9A) generally did not produce superior sorbents with the exception of experiment 7A for Np. Np sorption as it relates to sorbent preparation and characterization was counter to every trend observed for Sr and Pu sorption. In general (Figure 4), the peroxo-titanates prepared from the isopropanol-peroxide route were better sorbents for Np but poorer sorbents for Sr and Pu.

Further details concerning the disparate sorption behavior of Np can be observed in Figure 6. In this study, we compared Np, Sr, and Pu sorption kinetics for several dry-powder peroxo-titanate samples, along with the baseline MST slurry. These data predominately illustrate the effectiveness of a slurry sorbent compared to a dry powder sorbent in the case of Sr and Pu, and vice versa for Np. The three peroxo-titanates compared to baseline MST in this figure are (1) peroxo-titanate powder from an aqueous synthesis (1A), (2) a peroxo-titanate powder from an isopropanol synthesis (1I), and (3) peroxide-modified MST (6P), filtered and used as a dry powder. At 2 h solution contact time, the baseline MST slurry had adsorbed more Sr than 2 of the 3 peroxo-titanate

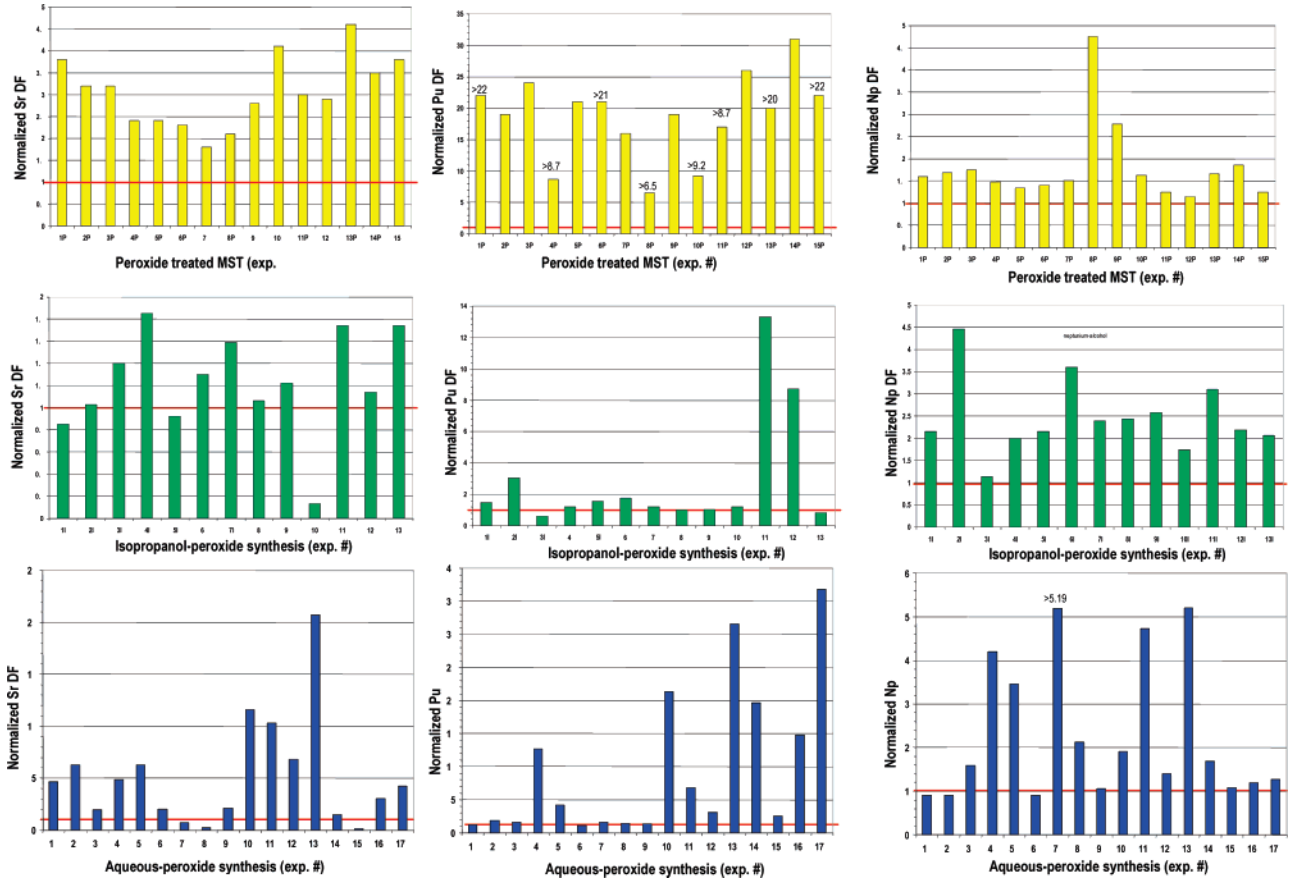

Figure 4. Summary of peroxo-titanate decontamination factors (DF) for strontium, plutonium, and neptunium normalized to DF values for baseline monosodium titanate (red line at unity in each graph). The peroxide-treated MST are the yellow bars, peroxo-titanates from the isopropanol-peroxide synthesis are represented by green bars, and the peroxo-titanates from the aqueous-peroxide route are blue bars.

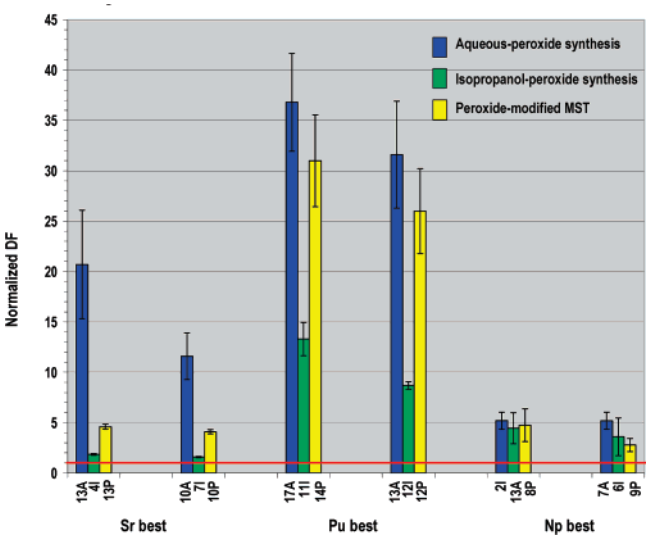

Figure 5. Bar graph comparing Sr, Pu, and Np decontamination factors (DF) of the best two peroxo-titanate sorbents for each of the three synthetic routes.

powders. However, with increased contact time (170 h), the three peroxo-titanate powders have removed more strontium than the baseline MST slurry.

The data for plutonium uptake is similar. At 2 h, the peroxo-titanate powders only slightly out-perform the baseline MST slurry. At 24 h, the three powder samples have removed more Pu than the baseline MST slurry; and at 170 h, two of the three powders show significantly better Pu removal data than the baseline MST slurry, and the third powder shows comparable performance to MST slurry.

Np sorption shows a different trend, with one powder sample (from the isopropanol preparation) showing significantly better performance at 2 h, and optimal performance for the powder samples at 24 h. However, at 150 h, the aforementioned peroxo-titanate from the isopropanol preparation has re-released some neptunium back into solution. In general, throughout 24 h, the peroxo-titanates did not show significant re-release of the radionuclide sorbates. At more than 170 h, the Sr and Pu did not exhibit any desorption, whereas partial desorption of Np is observed for some peroxo-titanate formulations.

Figure 7 provide plots of solution concentrations of strontium and plutonium upon contact with 0.1 and 0.2 g of MST/L for both baseline and peroxide-treated MST. The peroxo-titanate results are the average of duplicate tests for each of three peroxo-titanate samples. The three peroxo-titanate samples were prepared by the postsynthesis peroxide addition method (experiment 14P) at a larger scale (25 g versus 1.5 g for experiments 1P−15P listed in Table 1). Error bars in these figures are the single standard deviation of the six values for the peroxide-modified MST samples, the pooled single standard deviation of the six control samples taken over the entire test, and the analytical uncertainty reported for each sample measurement in the baseline MST test.

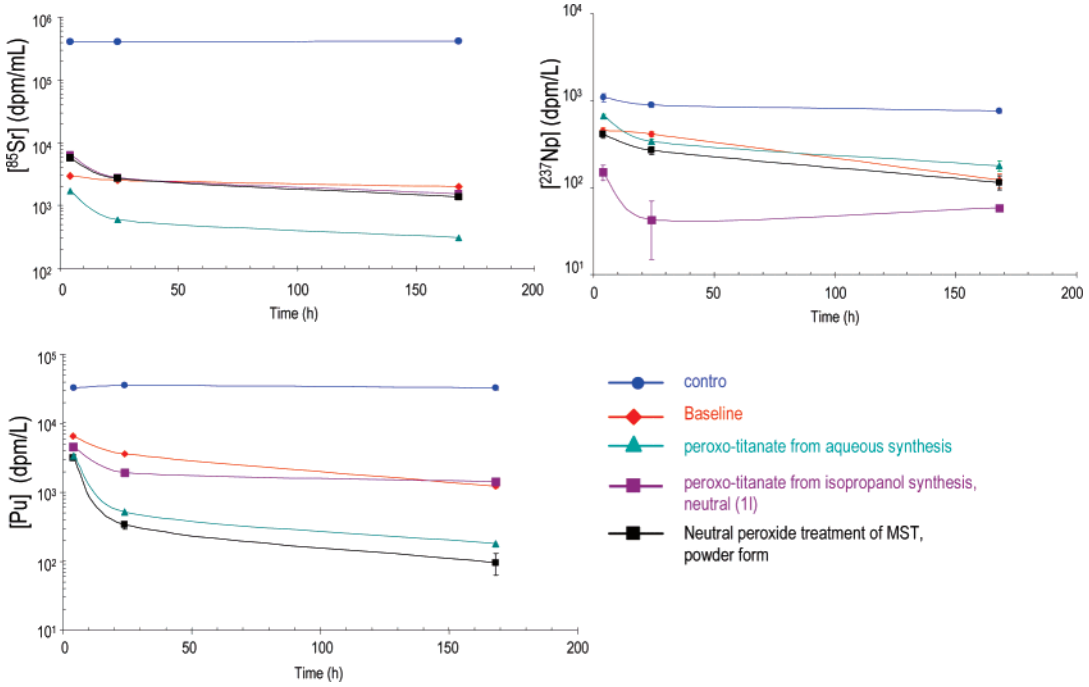

Figure 6. Plot of concentrations of Sr, Np, and Pu in Savannah River Site simulant with respect to time, in contact with sorbents. The concentration is measured in disintegrations per minute (dpm) per unit volume (per milliliter for Sr and per liter for Pu and Np). These graphs compare the performance of several dry-powder peroxo-titanates to that of baseline MST slurry. The control is the simulant without added titanate sorbent.

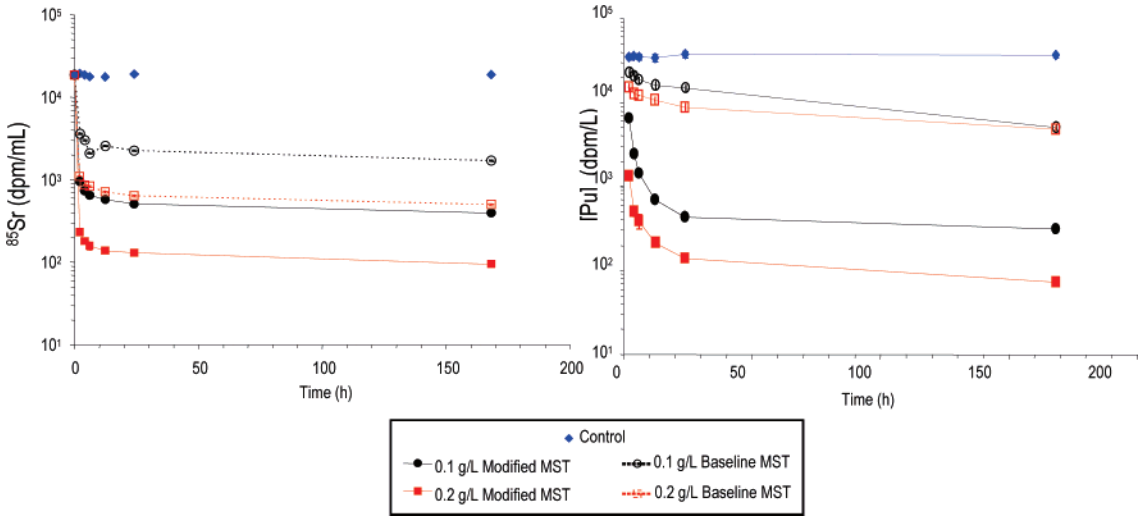

Figure 7. Plot of concentrations of Sr and Pu in Savannah River Site simulant with respect to time, in contact with MST slurry and peroxide-treated MST slurry, at two different sorbent concentrations. The concentration is measured in disintegrations per minute (dpm) per unit volume (per milliliter for Sr and per liter for Pu).

These tests show excellent reproducibility for the peroxo-titanate samples prepared at the larger scale and improved performance compared to the baseline MST. For strontium adsorption, doubling the amount of both baseline and peroxide-modified MST resulted in a proportional increase in strontium removal. However, the peroxide-modified samples removed more strontium than the baseline samples. Most of the strontium removal occurs during the first 2 h. The similarity of the four curves (in fact, two are overlapping) suggests that the strontium adsorption mechanism and the type of strontium sorption site does not change for MST upon peroxide modification. However, the number of available or accessible sites for strontium does increase upon peroxide modification.

The uptake of plutonium by MST and peroxide-modified MST shows differing behavior. Again, the peroxide-modified MST exhibits an overall improved Pu sorption rate and capacity over that of the baseline MST. The initial Pu sorption during the first 2 h is significant for all four tests. However, although Pu concentration in solution continues to decrease dramatically for the peroxide-modified MST up to 24 h, the sorption rate drops off for the baseline MST. Doubling the amount of baseline MST does not result in increased total Pu sorption near equilibrium (170 h), which suggests that at 0.2 g of MST/L, the baseline MST is saturated with respect to plutonium. However, doubling the amount of peroxide-modified MST does result in increased removal of Pu from solution. These results suggest the

Table 3. BET Surface Area and Normalized Sr, Pu, and Np DFs[a] for Selected Peroxo-titanate Samples

sample ID	surface area (m^2/g)	normalized Sr DF	normalized Pu DF	normalized Np DF
1A	73	4.64	1.25	0.91
2A	54	6.27	1.85	0.91
5A	251	6.25	4.16	3.46
6A	49	2.00	1.06	0.91
9A	46	2.14	1.34	1.06
baseline MST[b]	22.3	1	1	1
sample 14P-1	106	5.00	26.5	1.09
sample 14P-2	176	4.64	23.5	1.31
sample 14P-3	178	4.72	26.9	1.43

[a] Normalized DF values reported for 4 h contact time with stimulant, normalized to baseline MST (Optima batch 00-QAB-417). [b] Optima batch 00-QAB-417.

peroxide-modified MST has more Pu sorption sites available than baseline MST and the sorption mechanism and/or type of Pu coordination site does differ from that of baseline MST. Characterization and comparison of the Pu and Sr, as well as Np coordination sites in baseline MST[39] and peroxide-modified MST, are currently underway using XAFS (X-ray absorption fine structure spectroscopy) and vibrational spectroscopies (infrared and Raman).

Relationship between Peroxo-titanate Characteristics and Sorption Behavior. This investigation has revealed several important factors for optimizing sodium titanate sorbents for the removal of radionuclides from strongly alkaline nuclear wastes. Perhaps more importantly, the characteristics of the peroxo-titanates responsible for improved performance in these studies may be applied generally for other inorganic metal oxide sorbents, different target sorbates, and alternative sorption media. The most important findings include that (1) peroxo-titanate sorbents prepared or modified with hydrogen peroxide are universally superior to titanates prepared without hydrogen peroxide, (2) peroxo-titanate samples prepared, modified, or posttreated with acid are superior to their neutral or basic counterparts, and (3) drying sodium titanate sorbents at any time during the preparation or modification is deleterious to sorbent performance. Any of these points might be argued to be simply an effect of producing and retaining increased surface area, as well as more reactive surfaces. However, the poorly ordered nature of these sorbents challenges characterization of sorbate complexation, and we believe coordination of sorbates by peroxo-ligands may in fact contribute to enhanced sorption behavior.

Hydrogen peroxide plus acid or base are good mineralizing solutions for titania. Therefore, partial dissolution of the oxide upon exposure to these reagents can produce porosity and accessibility to sorption sites. For the isopropanol-peroxide syntheses and peroxide modification of MST, the combination of base and peroxide produced poorer performing sorbents than the analogous acidic or neutral treatments. Perhaps this is related to the different mechanisms of hydrolysis, condensation, and precipitation of oxides in acidic vs basic environments. Acidic conditions favor hydrolysis and thus the formation of high-surface-area, protonated powders, whereas basic conditions favor condensation and, therefore, produce more monolithic, deprotonated solids with lower surface area.[41]

We measured surface area of several peroxo-titanate samples, and these results along with normalized DF values for Sr, Pu, and Np are listed in Table 3 (sample IDs correspond with those in Table 1). Regarding the first five dry powder samples, the striking difference in the performance is the actinide DFs: 5A has considerably more surface area and is far superior for Pu and Np sorption, but is more comparable to the other samples for Sr removal. The main difference between 5A and the other four samples is a postsynthesis acidic treatment (see Table 1). The increased surface area may be a result of this pH adjustment (due to the mineralizer effect).

The improved actinide sorption may be linked simply to increased surface area and porosity, but is probably also related to the nature of the Ti-peroxo species stabilized under acidic conditions, because there was not a similar improvement in Sr sorption. Regarding the baseline MST and peroxide-modified MST, the surface areas of peroxide-modified MST are higher, corresponding with universal improvement in DF values. Another difference between the MST and treated MST samples is the pore size. The average pore size went from around 215 Å in the baseline MST to 30 Å in the peroxide-modified MST. It is likely that the 215 Å pores are interparticle space and the 30 Å pores represent porosity or accessible layering within the titanate material.

In the case of an ion-exchange mechanism of sorption (i.e., exchange of Na^+ or H^+ for Sr^{2+}), the acid forms of the sorbents have an advantage over the sodium forms, which may also contribute to the superior performance of sorbents post-treated with acid or synthesized in acidic media. That is, the hydronium ion is smaller than the hydrated sodium cation and, therefore, can exchange out from the titanate layers more readily, especially in the highly caustic waste solutions that contain a 1.3 M free hydroxide concentration (see Table 2). It has been observed in other ion-exchange materials that the protonated form has higher selectivity and faster exchange kinetics than alkali forms.[42,43]

We expect a sorbent that has never been dried to also have a more reactive surface and higher surface area. The surface oxygen sites of an oxide in water should be coordinatively saturated by aqueous species. On the other hand, an oxide that is dried will form bonds between surfaces via dehydration and thus lose both surface area and reactive sites for

(41) Brinker, C. J.; Scherer, G. W. *The Physics and Chemistry of Sol−Gel Processing*; Academic Press: Elsevier Science: San Diego, CA, 1989.

(42) Bortun, A. I.; Bortun, L. N.; Poojary, D. M.; Xiang, O.; Clearfield, A. *Chem. Mater.* **2000**, *12*, 294−305.

(43) Zheng, Z.; Phillip, C. V.; Anthony, R. G.; Krumhansl, J. L.; Trudell, D. E.; Miller, J. E. *Ind. Eng. Chem. Res.* **1996**, *35*, 4246−4256.

exchange. Returning a dry powder to an aqueous environment can reverse the process and regenerate reactive surfaces (albeit slowly), which is likely the phenomenon being observed in Figure 7. The peroxo-titanate powders are poorer or comparable sorbents to the baseline MST slurry at 2 h contact time but exceed MST performance with prolonged contact time. On the other hand, sorption by the MST slurry slows down significantly beyond 2 h. In summary, the uptake kinetics of a sorbent is much reduced by converting a slurry form to a dry powder, but not necessarily the equilibrium sorption capacity and selectivity.

Finally, we come to the issue of the peroxo species serving as ligands for the strontium and actinide sorbates. The peroxo ligand can exist as O_2^{2-}, HOO^-, or H_2O_2 and can be bound to titanium side-on or end-on.[38] Stable peroxo-actinide (predominantly uranium and neptunium) complexes are reported in both aqueous solutions and solid phases, including naturally occurring minerals for uranium.[44−48] Therefore, it is not unreasonable to expect these complexes to form between a sorbent containing peroxo ligands and sorbed actinides, thus contributing to the increased affinity of peroxo-titanates for actinides. As mentioned before, we are currently investigating the chemical environment of these sorbed actinides using XAFS and vibrational spectroscopies to determine if the peroxo groups have a significant role in the binding of these sorbates.

Conclusions

We have developed a new class of peroxo-titanate sorbents by three different synthetic methods. The peroxo-titanates exhibit improved performance compared to existing sodium titanate materials for the separation of strontium and actinides from highly alkaline and high-ionic-strength solutions. Testing also indicated that improved performance of these materials occurs when the peroxo-titanates are acidified and maintained in a fully hydrated form (e.g., as aqueous slurries). We believe the synthetic routes described in this paper can be extended to other transition metal-oxide sorbent systems, which we are actively investigating.

Finally, when Dosch first identified the prototype sodium titanate as a metal sorbent in the mid-70s, he noted its affinity for removing a whole host of metals, including lanthanides, alkaline earths, precious metals, and transition metals.[33] He also noted efficacy in various media, including acidic and basic aqueous solutions. Given the improved performance of the peroxo-titanates to separate strontium and actinides in simulated nuclear waste solutions, we have confidence that peroxo-titanates will exhibit improved separation characteristics for a variety of metal types and conditions. These studies, along with attempts to understand the mechanism of peroxo-titanate sorption, are ongoing.

Acknowledgment. This work was funded by the Department of Energy, Office of Environmental Management, by grants from the Office of Cleanup Technologies and the Office of Biological and Environmental Research in the Office of Science by a grant from the Environmental Management Science Program. Savannah River National Laboratory is operated by the Washington Savannah River Company for the U.S. Department of Energy's Office of Environmental Management under Contract DE-AC09-96SR18500. Sandia National Laboratories is a multiprogram laboratory operated by Sandia Corporation, a Lockheed Martin Company, for the U.S. Department of Energy's National Nuclear Security Administration under Contract DE-AC04-94AL85000. The authors thank Dr. Tom Headley and Dr. Chuck Hills (SNL) for the TEM and HR-TEM analyses and Dr. Ralph White and Dr. Chuck Holland, Department of Chemical Engineering, University of South Carolina, for selected surface area and porosimetry analyses. We also thank Dr. David DiPrete, Ms. Ceci DiPrete, and Mr. Curtis Johnson for the radiochemical analyses as well as Ms. Mona Blume and Ms. Kimberly Wyzsynski for performing the sorption tests at SRNL.

CM061797H

(44) Burns, P. C.; Kubatko, K.; Sigmon, G.; Fryer, B. J.; Gagnon, J. E.; Antonio, M. R.; Soderholm, L. *Angew. Chem., Int. Ed.* **2005**, *44*, 2135−2139.
(45) Gogolev, A. V.; Shilov, V. P.; Pikaev, A. K. *Mendeleev Commun.* 1996, 127−128.
(46) Kubatko, K.; Helean, K. B.; Navrotsky, A.; Burns, P. C. *Science* **2003**, *302*, 1191−1193.
(47) Shilov, V. P.; Gogolev, A. V.; Pikaev, A. K. *Mendeleev Commun.* 1998, 220−222.
(48) Shilov, V. P.; Gogolev, A. V.; Pikaev, A. K. *Radiochemistry* **1998**, *40*, 321−325.